

Topological analysis of graphoglyptid trace fossils, a study of macrobenthic solitary and collective animal behaviors in the deep-sea environment

Ruo-ying Fan, Yi-ming Gong, and Alfred Uchman

Abstract.—Graphoglyptids are biogenic structures commonly found in deep-sea flysch deposits and occasionally detected on the modern deep-sea floor. They extend principally horizontally and take a variety of geometric patterns, whose functional morphology remains an enigma in ichnology and paleoceanography. Based on published materials from 1850 to 2017 (79 ichnotaxa from 28 ichnogenera of graphoglyptids) and systematic observations of one of the largest deep-sea trace fossil collections in the world, this paper proposes that topological analysis is an important ingredient in the taxonomy and functional interpretation of graphoglyptids. Accordingly, graphoglyptids are classified into line, tree, and net forms by their key topological architecture, and are further attributed to 19 topological prototypes by detailed secondary topological features. Line graphoglyptids are single-connected structures with uniform tunnel width, representing primarily the feeding patterns of solitary animals. Tree graphoglyptids, the most diverse architectural group of graphoglyptids, are ascribed to 11 topological prototypes according to the connectivity features of burrow segments and the number and distributional pattern of the branching points. Net graphoglyptids are subdivided into three topological prototypes on the basis of the connectivity features and/or the regularity of the meshes. Multiconnected net forms are considered as a continuous morphological spectrum with different levels of complexity in the net formation. The various connected components in multiconnected tree and net graphoglyptids generally exhibit small and uniform tunnel diameter in a given structure (suggesting a tiny trace maker[s]). The whole structure shows relatively extensive linear or surface coverage and overall good preservation, indicating sustained processes of burrow construction. It is highly probable that certain multiconnected tree and net graphoglyptids represent some emergent patterns from self-organized collective behaviors of conspecific animals. Graphoglyptids thus provide us with a new perspective on the study of solitary and collective behaviors of macrobenthos in the deep-sea environment.

Ruo-ying Fan and Yi-ming Gong. *State Key Laboratory of Biogeology and Environmental Geology, School of Earth Sciences, China University of Geosciences, Wuhan 430074, China. E-mail: cugfry@163.com, ymgong@cug.edu.cn*

Alfred Uchman. *Institute of Geological Sciences, Jagiellonian University, Gronostajowa 3a, 30-387 Kraków, Poland. E-mail: alfred.uchman@uj.edu.pl*

Accepted: 26 December 2017
Published online: 6 March 2018

Introduction

“Graphoglyptid” is a loose term encompassing biogenic structures with patterned, regular, and complex morphology that are commonly found in deep-sea sediments from the Cambrian to the Recent (Fuchs 1895; Seilacher 1977; Ekdale 1980; Uchman 2003), with rapid radiation and diversification since the Late Cretaceous (Uchman 2003, 2004). Traditionally, they have been attributed to four major morphological groups (i.e., meandering, spiral, radial, and network structures) (Uchman 2003; Lehane and Ekdale 2014, 2016), with some more detailed geometric grouping (Seilacher 1977). As records of mostly deep-sea benthic animal activities near the sediment–water interface (Seilacher 1962), graphoglyptids may

offer a special perspective on the macrobenthic ecology and habitats in the deep-sea ecosystems (Ramirez-Llodra et al. 2010), yet remain a mystery as to their possible producers, constructional morphology, and paleoecology (Miller 1991, 2014). Deep-sea neoichnological study has made important progress during the last few decades, due to the development and popularization of deep sea–exploration devices, such as remotely operated vehicles, deep-submergence vehicles, and their mounted high-definition digital cameras and sampling tools (e.g., box corer). These new technologies have revealed a number of graphoglyptid-like structures on the modern deep-sea floor, including *Cosmorhapse*, *Helminthorhapse*, *Lorenzinia*, *Paleodictyon*, *Spirorhapse*, and *Urohelminthoida*

(Heezen and Hollister 1971; Ekdale 1980; Gaillard 1991; Rona et al. 2009; Przeslawski et al. 2012; Bell et al. 2013; Durden et al. 2017). Nevertheless, these frequently encountered representatives contrast with the immense morphological diversity of graphoglyptids in the fossil record. However, an active graphoglyptid maker has never been identified by deep-sea photography or neoichnological researches (Rona et al. 2009). Although shallow-marine graphoglyptid finds do exist in the fossil record (e.g., Fürsich et al. 2007; Olivero et al. 2010), modern shallow-marine in situ or laboratory studies fall short in revealing comparable animal architectures. A number of studies have summarized the current knowledge of the abundance, biomass, and diversity of the modern deep-sea benthos (e.g., Rex et al. 2006; Danovaro et al. 2010), but less attention is paid to their in situ behaviors. A handful of studies examined the production of meandering trace fossils using computer simulation or in a laboratory setting (Koy and Plotnick 2007, 2010; Sims et al. 2014); however, for the most part, graphoglyptids remain an enigma in deep-sea ichnology, sedimentology, and paleoceanography and deep-ocean ecology. Understanding of their functional and ecological implications still relies largely on the investigation of fossil materials.

In the traditional morphometric study of trace fossils, the problem of morphological gradation cannot be avoided, and the selection of end members is more or less arbitrary (Miller 2012). Trace fossils generally display particular burrow architectures, which are even more distinct in the patterned graphoglyptids. The understanding of the essential morphological features (i.e., the layout of burrow systems and the relative spatial arrangement of different burrow segments) is crucial in the functional interpretation of graphoglyptids. In this respect, the application of the theories of topology, which considers the properties of objects under continuous deformation, would be beneficial to find out the essential morphological constructs of complex geometric patterns (cf. Gong and Si 2002; Lehane and Ekdale 2014).

This paper reports on a comprehensive morphological study of graphoglyptids by

means of topological analysis. Theoretical morphotypes (topological prototypes) are established for all graphoglyptids. From these, probable solitary and collective behaviors of deep-sea benthic macrofauna are suggested. The analytical procedures proposed in this paper may provide some theoretical bases and practical cases for studying complex trace fossils and organism–environment interactions in the deep ocean.

Materials and Methods

Materials.—Based on systematic monographs on deep-sea trace fossils (e.g., Książkiewicz 1977; Seilacher 1977; Uchman 1995, 1998, 1999, 2001) and shorter systematic papers (according to the deep-water flysch ichnological records from Uchman [2004] and Lehane and Ekdale [2016]), we conducted a comprehensive morphological study of graphoglyptids published from 1850 to 2017. Valid graphoglyptid ichnotaxa were adapted from summaries of Uchman (2003) and Buatois et al. (2017). Detailed supplementary observations were carried out on the Late Cretaceous to Miocene deep-sea trace fossil collections (Marian Książkiewicz's and Alfred Uchman's collections, specimen prefixes UJ TF and 143P/144P/149P/171P/173P/179P, respectively) deposited at the Nature Education Centre of the Jagiellonian University–Museum of Geology, Kraków, Poland.

Basics and Methodology of Topological Analysis.—The methods of topology have been previously applied to the study of trace fossils (Gong and Si 1991, 2002; Gong and Huang 1997; Huang and Gong 1998). Topology is the branch of mathematics that studies the properties of space under continuous deformation. Continuous deformation or topological deformation is deformation such as stretching, crumpling, and bending, but not tearing or gluing. The topological invariant is defined as the invariant attributes of a given figure during the process of topological deformation. If two figures can transform to each other after continuous deformation, they are called homeomorphic. For example, a sphere surface, a cubic surface, and an irregular closed surface are all homeomorphic.

The major parameters used in the topological analysis of graphoglyptids follow those of

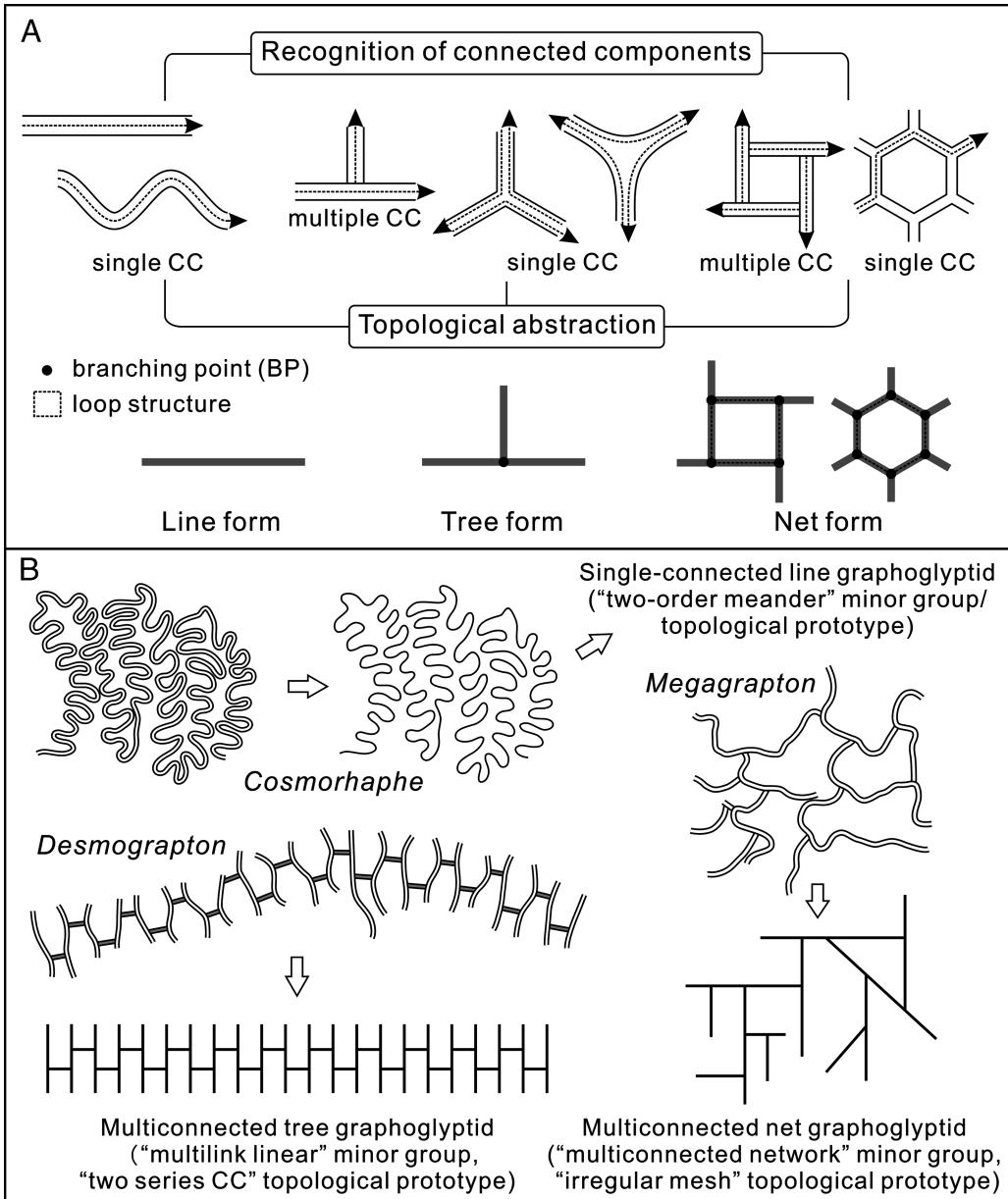


FIGURE 1. Methodology and examples of topological analysis of trace fossils. A, Topological structure analysis enveloping two aspects of connected component recognition and topological abstraction, broadly dividing graphoglyptids into three distinct groups: line, tree, and net forms. B, Examples of topological analysis of typical graphoglyptids (with major and minor groups as well as topological prototypes indicated), shapes of *Cosmorhaphe*, *Desmograpton*, and *Megagraption* traced from Seilacher (1989: Fig. 1), Fuchs (1895: Plate 5, Fig. 6), and UJ TF 793, respectively.

Gong and Si (2002), of which the most important concepts are the connected component and the branching point (Fig. 1A). The topological analysis of trace fossils envelops two aspects: the recognition of connected components and the identification of the

organization of branching points through topological abstraction (Fig. 1A). For major topological grouping, we focus on the abstracted topological structure and the general arrangement of the branching points, dividing trace fossil architectures into line, tree, and net

forms (Fig. 1A). For finer-scale topological characterization, the connected component features and the detailed arrangement of the branching points in a given pattern should be taken into consideration (Fig. 1B).

By definition, the connected part of a given pattern is denoted as its connected component (CC) and the branching point (BP) is the point where three or more burrow parts are attached. Line-form trace fossils are essentially made of a single connected component (Fig. 1A). The recognition of connectivity at the branching points of tree and net forms may be ambiguous, because preservation states may affect and smooth certain morphological details. However, certain rules of thumb may be applied. Suppose a branched structure (tree and net form alike) is single-connected (meaning all the burrow branches can be traversed freely by the trace maker[s]), then multiple recrossing at the branching point may induce enlargement there. The swellings at the T- or Y-shaped burrow conjunctions commonly found in the trace fossil *Thalassinoides* are a good example of such “recrossing features” at the branching point of single-connected branched structures (Bromley and Frey 1974). Therefore, if there is enlargement or the various branches are well fused at the branching points, the branched structure is considered single-connected (Fig. 1A). Conversely, if there is no enlargement at the branching point and if there are several well-defined and coherent burrow segments around the branching point, the branched structure is considered multi-connected (Fig. 1A).

Based on the detailed topological features of trace fossils, several ichnotaxa may be composed of a common topological structural pattern corresponding to a specific set of topological parameters and/or morphological details; this is the basis of minor topological grouping (Fig. 1B). A minor topological group may be subdivided into several topological prototypes according to variations in certain morphological details. The topological prototypes thus stand as the lowest rank in the topological classification scheme and may be seen as “topological *Bauplans*” representing particular construction styles of a certain group of trace fossils. In this way, the minor topological grouping or the topological

prototype of a given trace fossil is a purely morphology-based property and can be well incorporated as a part of ichnotaxobases sensu Bertling et al. (2006).

It should be noted that the syndepositional and/or diagenetic processes commonly exert certain deformations to the trace fossils preserved in sediments in various ways (see recognition of distortion in trace fossils by Monaco [2008]). Therefore, the complete topological analysis should first of all (as a prerequisite) identify the possible morphological distortion from syndepositional or diagenetic deformations (see also notes for Table 1). It is only after this step that the topological analysis of the original morphology of the trace fossils can be undertaken.

Results

The published graphoglyptid trace fossils (1850–2017, 28 ichnogenera and 79 ichnospecies) are divided into three major topological groups, i.e., line, tree, and net graphoglyptids (cf. Gong and Si 2002; Lehane and Ekdale 2014), which are subdivided into 13 minor topological groups and further attributed to 19 topological prototypes (Table 1).

Topological Architecture and Prototypes of Line Graphoglyptids.—Line graphoglyptids are represented by a moderate number of ichnotaxa (14 ichnospecies) (Table 1). The line graphoglyptids share a common set of topological parameters (CC = 1, BP = 0) and are subdivided into five minor groups according to the presence or not of multiple-scale meandering and the rotation direction and orientation of the spiral burrow parts (Table 1, Fig. 2G). Each of the topological patterns of the five minor groups signifies a distinct topological prototype.

The “one-order meander” topological prototype (L-1) is well represented by *Helminthorhapha*, which exhibits only one order of systematic meander (Seilacher 1977; Uchman 1995; Fig. 2A). The morphospace of *Helminthorhapha* has been characterized by the meander width and the fractal dimension of the meandering pattern (Fan et al. 2017). “Two-order meanders” (L-2) are most prominent in *Cosmorhapha* (Fig. 2B). “One-way spiral” structures (L-3) include *Spirorhapha azteca* Seilacher,

TABLE 1. Topological classification scheme of all graphoglyptid trace fossils (3 major groups, 13 minor groups, and 19 topological prototypes). Identification format such as “L-1/One-order meander” in the first column means the number and name of the minor group (it happens that the topological prototype and the minor group are the same in the case of some less diverse line and tree graphoglyptid categories, in which the number is italicized); abbreviations L, B, and N are for line-, tree-, and net-form graphoglyptids, respectively. Identification format such as “B-4-1 (straight or gently curved series)” in the second column indicates the number and name of the topological prototype. Abbreviations of topological parameters: CC, connected component; BP, branching point (see details in “Materials and Methods”).

| Minor topological groups | Graphoglyptid ichnotaxa |
|---|--|
| L-1/One-order meander: CC = 1, BP = 0 | <i>Helminthorhapha flexuosa</i> , <i>H. japonica</i> , <i>H. miocenica</i> , <i>H. reflecta</i> , <i>H. magna</i> |
| L-2/Two-order meander: CC = 1, BP = 0 | <i>Cosmorhapha lobata</i> , ¹ <i>C. sinuosa</i> , <i>C. gracilis</i> , <i>Spirocosmorhapha labyrinthica</i> ² |
| L-3/One-way spiral: CC = 1, BP = 0 | <i>Spirorhapha azteca</i> , <i>S. graeca</i> |
| L-4/Two-way spiral: CC = 1, BP = 0 | <i>Spirorhapha involuta</i> |
| L-5/Lateral spiral: CC = 1, BP = 0 | <i>Helicolithus sampelayoi</i> , <i>Helicorhapha tortilis</i> |
| B-1/Stellate: CC = 1, BP = 1 | <i>Estrellichnus jacaensis</i> , ? <i>Glockerichnus disordinata</i> , ? <i>G. parvula</i> , ? <i>G. sparsicostata</i> |
| B-2/Twiggly stellate: CC = 1, BP ≥ 4, BPs forming tree topology | <i>Chondrorhapha bifida</i> , <i>Glockerichnus glockeri</i> , <i>G. alata</i> (tentatively), <i>G. dichotoma</i> , <i>Dendrorhapha haentzscheli</i> ³ |
| B-3/Branched zigzag: CC = 1, BP ≥ 2, BPs forming line topology but arranged separately on each branch | <i>Urohelminthoidea appendiculata</i> , <i>Helicolithus ramosus</i> (tentatively) |
| B-4/Uniserial branch: CC = 1, BP ≥ 2, BPs forming line topology and aligned in a series on a main stretch of various morphology | B-4-1 (straight or gently curved series): <i>Acanthorhapha delicatula</i> , <i>A. incerta</i> , <i>Protopaleodictyon spinata</i> , <i>Ubinia wassoevitschii</i> B-4-2 (semicircular series): <i>Persichnus dodecimanus</i> B-4-3 (spiral series): <i>Yakutatia emersoni</i> B-4-4 (meandering series): <i>Belorhapha zickzack</i> , <i>Protopaleodictyon incompositum</i> , <i>P. minutum</i> |
| B-5/Multilink linear: CC ≥ 3, BP ≥ 2, BPs forming line topology but arranged separately on each CC | B-5-1 (L- or U-shaped CC): <i>Arabesca simplex</i> , <i>A. cervicornis</i> , <i>A. caucasica</i> , <i>A. daghestanica</i> , <i>Ubinia alternans</i> B-5-2 (straight or gently undulated CC): <i>Urohelminthoidea dertonensis</i> B-5-3 (two series CC): <i>Belocosmorhapha aculeata</i> , ⁴ <i>Desmograption dertonensis</i> , <i>D. alternum</i> , <i>D. ichtyforme</i> , <i>D. pamiricus</i> , <i>Helicolithus tortuosus</i> , <i>Oscillorhapha venezuelana</i> (tentatively), <i>O. italica</i> (tentatively), <i>Paleomeandron elegans</i> , <i>P. rude</i> , <i>P. robustum</i> , <i>P. biserialis</i> , <i>P. transversum</i> , <i>Protopaleodictyon bicaudatum</i> (tentatively) |
| ?B-6/Multiconnected loop: CC ≥ 8 (mostly), untouched, arranged in a semicircular fashion | <i>Capodistria vetteri</i> , <i>Fasciclichnus extentum</i> , <i>Lorenzina apenninica</i> , <i>L. kuzniari</i> , <i>L. carpathica</i> , <i>L. nowaki</i> , <i>L. plana</i> , ? <i>L. pustulosa</i> |
| N-1/Single-connected network: CC = 1, BP ≥ 2, BPs forming loop topology | N-1-1 (irregular mesh), N-1-2 (regular mesh), N-2 (multiconnected network) ⁵ : <i>Megagraption submontanum</i> , <i>M. irregulare</i> , <i>Paleodictyon petaloideum</i> , <i>P. tectiforme</i> , <i>P. minimum</i> , <i>P. latum</i> , <i>P. strozzii</i> , <i>P. miocenicum</i> , <i>P. delicatulum</i> , <i>P. majus</i> , <i>P. goetzingeri</i> , <i>P. maximum</i> , <i>P. arvense</i> , <i>P. croaticum</i> , <i>P. hexagonum</i> , <i>P. italicum</i> , <i>P. gomezi</i> |
| N-2/Multiconnected network: CC ≥ 2, BP ≥ 2, BPs forming loop topology | |

¹Among all the *Cosmorhapha* ichnospecies, *C. lobata* Seilacher, 1977 (first reported in Fuchs [1895: Plate 6, Fig. 5]) stands as the most typical of the defined behavior, showing deep and distinct second-order meanders. *Cosmorhapha sinuosa* (Azpeitia Moros, 1933) occasionally exhibits short appendages near the apex of the second-order meander (see Seilacher [1977: Fig. 4a, b]; specimens UJ TF 242, 243), making it more akin to *Protopaleodictyon incompositum* Książkiewicz, 1970 in the topological architecture. *Cosmorhapha gracilis* Książkiewicz, 1977 is similar to *C. sinuosa* in having relatively shallow second-order meanders, but is generally smaller and not associated with lateral appendages. *Cosmorhapha helminthoidea*, *C. neglectens*, *C. tremens* sensu Seilacher (1977), and *C. carpathica* sensu Uchman (1998) are essentially long meanders similar to *Helminthorhapha*; the irregular undulations of the meanders are best seen as irregularities of low taxonomical importance rather than the second-order meandering behavior. Only a slight change in the behavioral control could produce such irregular undulations in *Helminthorhapha* (Fan et al. 2017).

²*Spirocosmorhapha labyrinthica* (Heer, 1877) shows enlarged second-order meanders, which locally deviate from the smooth meander shape to take a branched structure (Seilacher 1989; Wetzel and Bromley 1996). However, based on an analysis of possible deformational effects from the diagenetic history, such branched structures could be created when oblique deformation took place, inducing displacement of the original burrow and rearrangement of the broken segments (discontinuous or nontopological deformation). Therefore, we consider it to be similar to *Cosmorhapha* as a two-order meander.

³The twiggly-stellate topological structure of *Dendrorhapha haentzscheli* (Farrés, 1967) is inferred, because the central part of the pattern is generally not preserved. However, the radial arrangement of several branched segments indicates that they probably emanate from a single central point (see Seilacher [1977: Fig. 10f]; Uchman [1999: Fig. 8A]).

⁴*Belocosmorhapha aculeata* (Książkiewicz, 1977) could tentatively be seen as a flattened form of *Paleomeandron*, which could be related to vertical pressing and horizontal extensional effects from continuous deformation in the diagenetic process (topological deformation).

⁵For network forms, it is not always easy to detect the connectivity features at the many branching points. It is common to find both connected and unconnected branched structures in a given pattern. The preservation biases cannot be completely removed, and the morphological details at the branching points may have been smoothed at least locally. Some net forms may be more properly assigned to only one type of connectivity features, e.g., *Megagraption irregulare* Książkiewicz, 1968 appears to be single-connected for most cases. And the highly regular “*Paleodictyon nodosum*” on the modern deep-sea floor has been proved to be a three-dimensional, single-connected structure (although its affinity to macrofaunal activities is not certain; see Rona et al. [2009]; Dürden et al. [2017]). *Paleodictyon* made of regular arrays of identical hexagonal meshes (e.g., *Paleodictyon minimum* Sacco, 1888, *P. miocenica* Sacco, 1886, *P. hexagonum* Van der Marck, 1863, as well as some forms of *P. strozzii* Meneghini in Savi and Meneghini, 1850) are essentially single-connected, which may be fossil examples of modern deep-sea, three-dimensional, hexagonal galleries. Traditionally, *Paleodictyon* ichnospecies have been characterized mostly by morphometric parameters such as tunnel diameter and mesh size (Uchman 1995) and the regularity or morphology of the meshes (e.g., irregular, petaloideal meshes found in *Paleodictyon petaloideum*, *P. tectiforme*, introduced as the subichnogenus *Squamodictyon* by Seilacher [1977]), but less on the connectivity features of the meshes. For a given *Paleodictyon* ichnospecies, there may be single- or multiconnected forms. Therefore, we are not able to separate the ichnotaxa for the three topological prototypes recognized for net graphoglyptids, and they are listed altogether.

1977 and *S. graeca* Seilacher, 1977 (Fig. 2C, D), which are similar to the non-graphoglyptid *Spirodesmos* (Huckriede 1952) in morphological

design (an Archimedes’ spiral, or arithmetic spiral, showing a constant separation distance between successive turnings intersected by

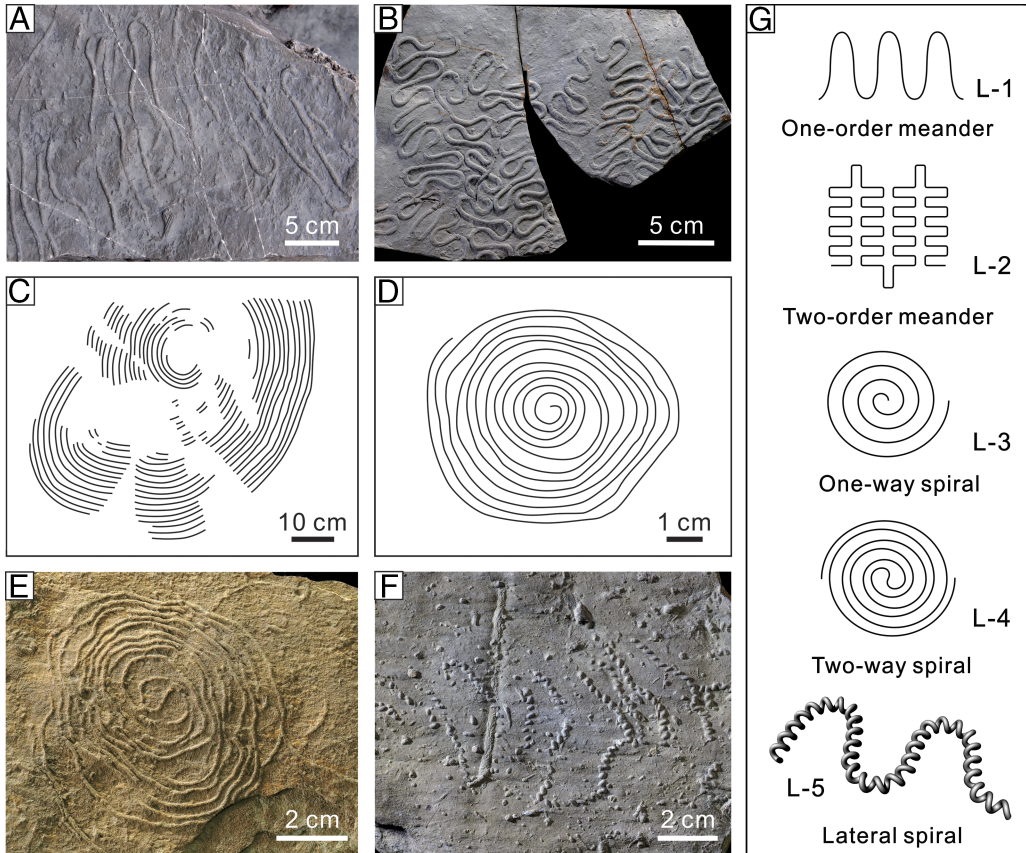


FIGURE 2. Topological architecture and prototypes of line graphoglyptids. A–F, Fossil examples of line graphoglyptids. A, *Helminthorhapse magna* Fan et al., 2017, field photograph, Campanian–Paleocene, Ropianka Formation, Słopnice, Carpathians, Poland. B, *Cosmorhapse lobata* Seilacher, 1977, Paleocene–lower Eocene, Variegated Shale, Lipnica Wielka, Carpathians, Poland, UJ TF 2684. C, *Spirorhapse graeca* Seilacher, 1977, Eocene, Pindos, Greece, traced from Seilacher (1977: Fig. 3m). D, *Spirorhapse azteca* Seilacher, 1977, Eocene, Tacanhuite, Mexico, traced from Seilacher (1977: Fig. 3l). E, *Spirorhapse involuta* (de Stefani, 1895), Eocene, Cieżkowice Sandstone, Górddek n. Dunajcem, Carpathians, Poland, UJ TF 211. F, *Helicolithus sampelayoi* Azpeitia Moros, 1933, upper Eocene, Magura Sandstone, Homrzska, Carpathians, Poland, UJ TF 227. G, Topological prototypes of line graphoglyptids enveloping five categories of one-order meander, two-order meander, one-way spiral, two-way spiral, and lateral spiral.

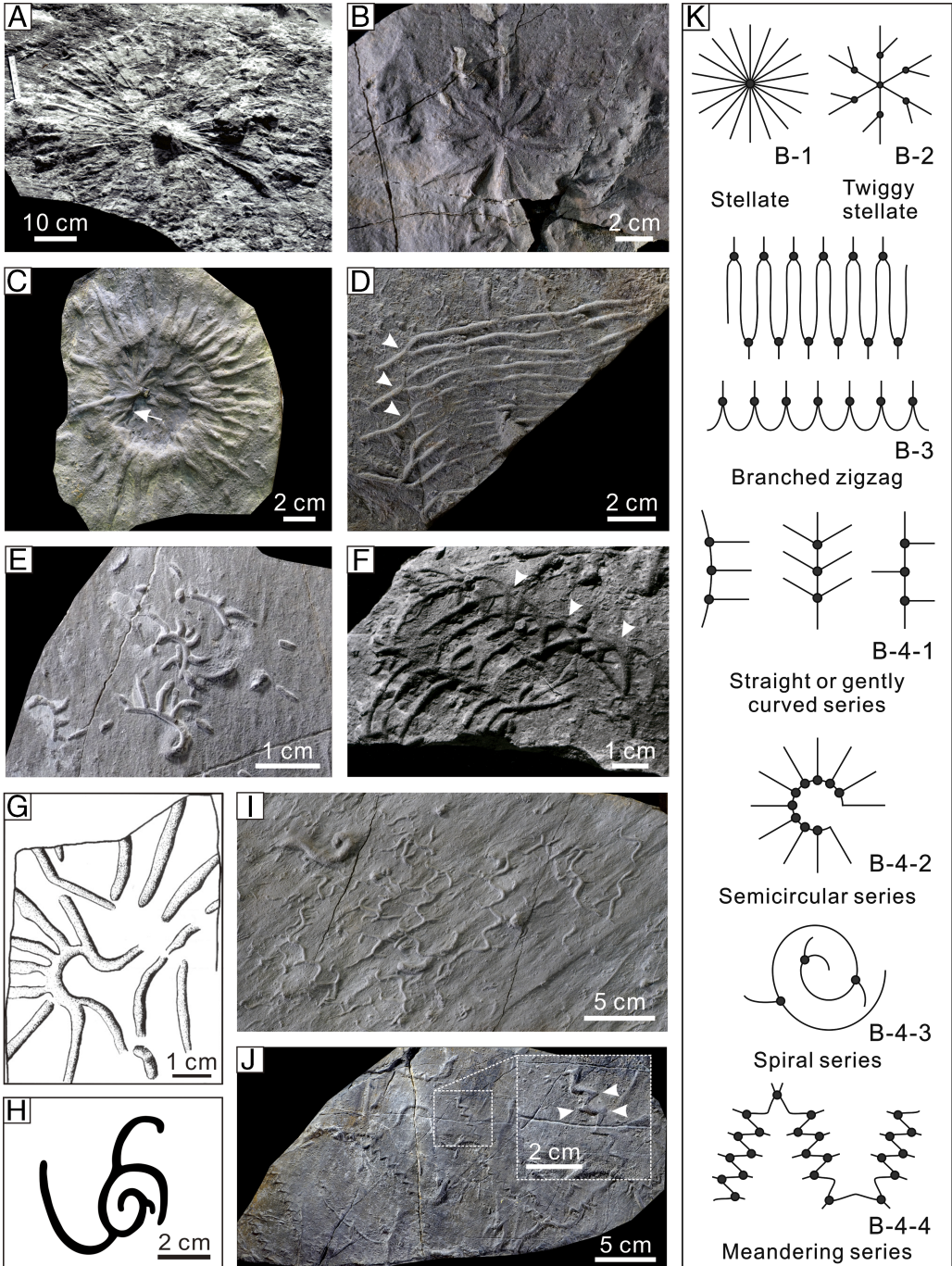
rays from the origin). These two ichnospecies have seldom been reported since their erection in Seilacher (1977). Tentative *Spirorhapse azteca* with high geometric order and numerous rings has also been found in the early Permian intertidal flat deposits (Minter et al. 2006), which shows striking similarity to the modern intertidal flat spiral-shaped burrows made by the paraonid polychaete *Paraonis fulgens* (Levinsen). The “two-way spiral” subgroup (L-4) consists of only one ichnotaxa, *Spirorhapse involuta* (de Stefani, 1895) (Fig. 2E), which conforms to the design of Fermat’s spiral (a spiral made of two identical connected spiral

limbs showing point symmetry). The “lateral spiral” category (L-5) includes *Helicolithus sampelayoi* Azpeitia Moros, 1933 and *Helicorhapse*, which are easily distinguished from the former four subgroups of essentially horizontally extended structures. Particularly, *Helicolithus sampelayoi* displays an organization of the lower-level lateral spirals in a higher-order meandering fashion (Fig. 2F).

Topological Architecture and Prototypes of Tree Graphoglyptids.—Tree graphoglyptids are a major topological architectural group of graphoglyptids, represented by 6 minor topological groups and 11 topological

prototypes from 48 ichnospecies (Table 1). They display a wide array of morphotypes depending on the connected component features, as well as the number and hierarchy of the branching points.

The “stellate” (B-1) and “twiggy-stellate” (B-2) topological prototypes are essentially single-connected structures, which differ by the presence or not of a hierarchy of the branching points (Table 1, Fig. 3K). The stellate topological



prototype (B-1) has only one branching point from which numerous branches emanate, which is best represented by *Estrellichmus jacaensis* Uchman and Wetzel, 2001, with its spoke-like radiating branches, and some forms of *Glockerichmus* (Table 1, Fig. 3A, B). The twiggy-stellate topological prototype (B-2) is characterized by a hierarchical arrangement of the branching points ($BP \geq 4$, Fig. 3K). The bouquet-like graphoglyptid trace fossils *Chondrorhaphae* and *Glockerichmus glockeri* (Książkiewicz, 1968) fall into this subgroup (Fig. 3C). The “branched-zigzag” topological prototype (B-3) is represented by *Urohelminthoidea appendiculata* (Heer, 1877), which shows long and tight hairpin turns with commonly enlarged and wider apex extensions (Fig. 3D), suggesting also a single-connected form. *Helicolithus ramosus* (Vialov, 1971) may be tentatively included in this prototype based on its three-dimensional reconstruction as allied, vertical U-shaped elements proposed by Seilacher (1977) (see Fig. 3K).

The “uniseriate branch” minor group (B-4) is represented by a moderate number of ichnotaxa (nine ichnospecies, Table 1). In this category, several burrow branches adhere to a main tunnel (just like leaves on a stem) ($BP \geq 2$, Table 1, Fig. 3K). As the morphology of the main tunnel shifts from straight, to curved, to circular, to spiral, and even to meandering, and the lateral appendages change from unilateral, to bilateral, and to alternate-sided, taking on a straight or curved shape, a spectrum of burrow-system morphologies could be envisaged. Each of the distinct main-tunnel morphologies can be

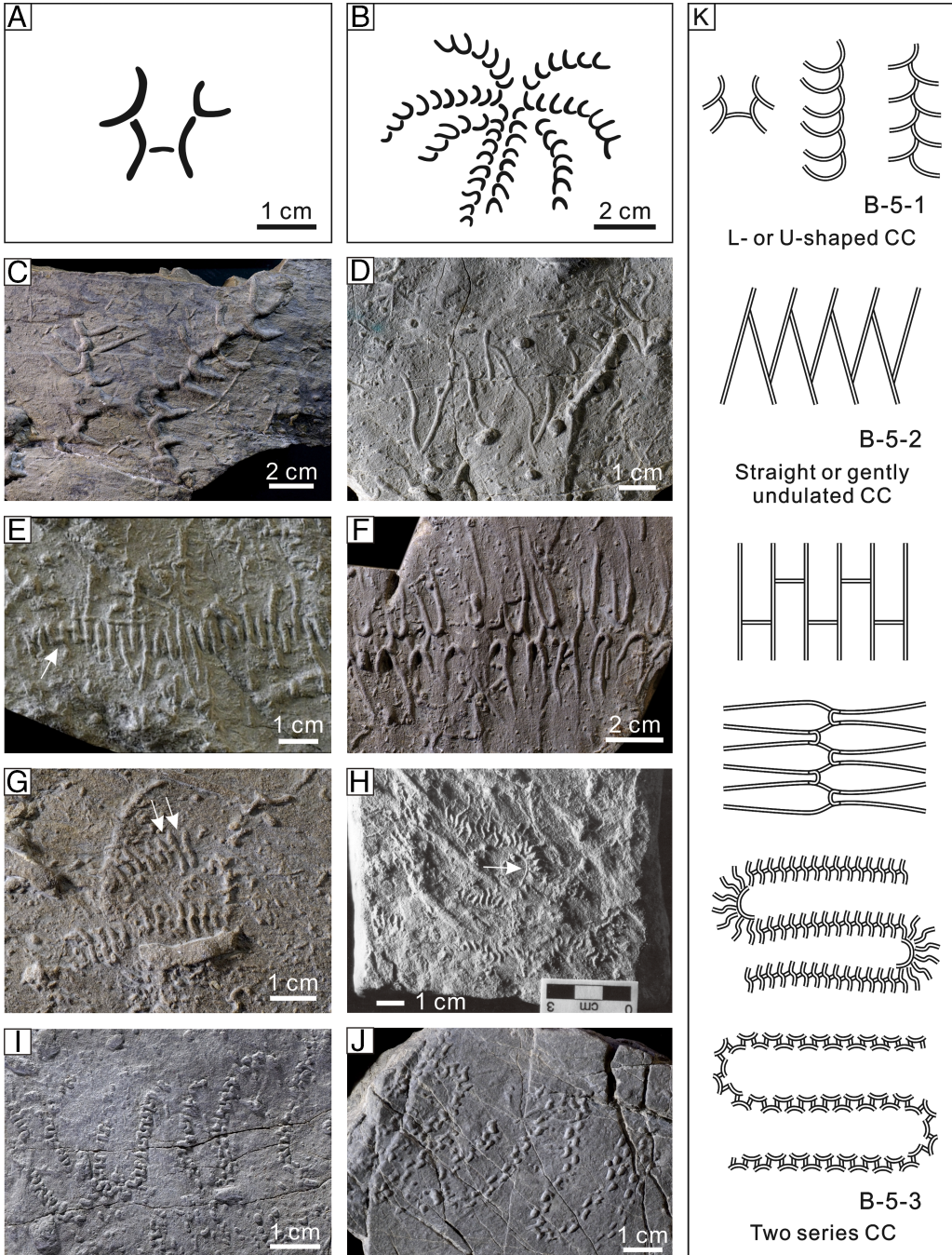
designated a topological prototype (Table 1, Fig. 3K). For example, the typical arch-shaped *Acanthorhaphae*, where several shorter burrow limbs attach single-sidedly to the longer, curved main tunnel (Fig. 3E), or *Ubinia wassoevitschi* Grossgeim, 1961 (Fig. 3F), with a straight main tunnel and bilateral or alternate curved appendages, are assigned to the “straight or gently curved series” topological prototype (B-4-1). The “semicircular series” (B-4-2) and “spiral series” (B-4-3) topological prototypes are relatively uncommon in graphoglyptids, each represented by only one ichnotaxa: *Persichmus dodecimanus* (Grossgeim, 1946) and *Yakutatia emersoni* (Ulrich, 1904) (Fig. 3G, H). There are certain forms where the main tunnel extends in a meandering fashion (B-4-4), typically in *Belorhaphae zickzack* (Heer, 1877) and *Protopaleodictyon incompositum* (Książkiewicz, 1970) (Fig. 3I, J, K). The “uniseriate branch” subgroup is also essentially single-connected. The enlarged apex of the zigzags in *Belorhaphae zickzack* is suggestive of multiple recrossing at the branching point (Fig. 3J). The lateral appendages in *Acanthorhaphae* and *Persichmus* are also well fused with the main tunnel, without distinct demarcation between the two (Fig. 3E, G).

The “multilink linear” minor group (B-5) is another distinct category of tree graphoglyptids (represented by 20 ichnospecies, Table 1). Hence the multilink linear topology is probably an important architectural design of tree graphoglyptids. This subgroup is made of successively linked or touching, well-defined burrow segments ($CC \geq 3$, multiconnected),

FIGURE 3. Topological architecture and prototypes of single-connected tree graphoglyptids. A–J, Fossil examples of single-connected tree graphoglyptids. A, *Estrellichmus jacaensis* Uchman and Wetzel, 2001, field photograph, holotype, Eocene, Hecho Group, Jaca, Spain, MPZ 98/477 (Museo Paleontológico de la Universidad de Zaragoza). B, *Glockerichmus sparsicostata* (Książkiewicz, 1968), Campanian–Paleocene, Ropianka Formation, Zawoja, Carpathians, Poland, UJ TF 210. C, *Glockerichmus glockeri* (Książkiewicz, 1968), second-order branching indicated, holotype, Berriasian, Cieszyn Limestone, Golezów, Carpathians, Poland, UJ TF 95. D, *Urohelminthoidea appendiculata* (Heer, 1877), enlarged apex extensions indicated, Campanian–Paleocene, Ropianka Formation, Lipnica Wielka, Carpathians, Poland, UJ TF 1592. E, *Acanthorhaphae delicatula* Książkiewicz, 1977, lower Eocene, Beloveža Formation, Lipnica Mała, Carpathians, Poland, UJ TF 1322. F, *Ubinia wassoevitschi* Grossgeim, 1961, note the overlapping of the lateral branches, Coniacian–Campanian, Yemişliçay Formation, Bürenük, Sinop-Boyabat Basin, Turkey, 173P10, from Uchman et al. (2004: Fig. 17H). G, *Persichmus dodecimanus* (Grossgeim, 1946), Upper Cretaceous to Eocene, Sanandaj, Iran, MMTT-318 (National Natural History Museum of Iran in Tehran), from Uchman et al. (2005: Fig. 2D). H, *Yakutatia emersoni* (Ulrich, 1904), holotype, Upper Cretaceous, Alaska, traced from Seilacher (1977: Fig. 9k). I, *Protopaleodictyon incompositum* Książkiewicz, 1970, middle Eocene, Hieroglyphic Beds, Osielec, Carpathians, Poland, UJ TF 130. J, *Belorhaphae zickzack* (Heer, 1877), enlarged zigzag apexes and local branching from the apex indicated in the inset, which indicate the original presence of branches attached to the apexes of the zigzag route and recrossing-induced swelling at the branching points, Valanginian, Upper Cieszyn Shales, Jaroszwice, Carpathians, Poland, UJ TF 119. K, Topological prototypes of single-connected tree graphoglyptids (a total of seven, rounded dots represent branching points).

and the branching points are distributed on the individual burrow segments ($BP \geq 2$, Table 1, Fig. 4K). According to the morphology of the individual connected components and their specific arrangement styles, the multilink linear subgroup can be ascribed to three

distinct topological prototypes (Table 1, Fig. 4K). Several L- or U-shaped burrow segments connected one after another to form the topological prototype B-5-1, which is represented by *Arabesca* ichnospecies and *Ubinia alternans* (Seilacher, 1977) (Fig. 4A–C).



The orientation of the L- or U-shaped burrow segments may be horizontal or slightly oblique to the bedding surface. Predominantly straight horizontal burrow segments touch one by one to produce *Urohelminthoidea dertonensis* Sacco, 1888 (B-5-2, Fig. 4D). Several other ichnotaxa, for example, *Helicolithus tortuosus* (Książkiewicz, 1970), *Paleomeandron*, and *Desmograption*, exhibit distinct geometric patterns and are composed of similar structural elements, which are here attributed to the topological prototype “two-series connected component” (Table 1, Fig. 4E–J). This topological prototype is made up of two connected component series, the semiparallel tube series and the alternate connecting-tunnel series (Fig. 4K). The two series of burrow segments are likely distributed along surfaces with a minor depth difference, as evidenced by a slight elevation difference between the two series. Specifically, *Desmograption* consists of long semiparallel tubes and straight or U-shaped connecting tunnels (Fig. 4E, F). There is considerable morphological variety inside *Desmograption*: *D. ichthyforme* (Macsoy, 1967) displays straight semiparallel tubes and straight connecting tunnels (Fig. 4E), whereas *D. dertonensis* (Sacco, 1888) and *D. alternum* (Książkiewicz, 1977) (Fig. 4F) exhibit regularly flexing semiparallel tubes and U-shaped connecting tunnels. *Helicolithus tortuosus* is composed of S-shaped, short, semiparallel tubes and straight connecting tunnels, which are organized in an overall meandering pattern (Fig. 4G, H). *Paleomeandron* is made of minute parallel tubes and flattened U-shaped connecting tunnels (Fig. 4I, J). *Paleomeandron*

is similar to *Helicolithus tortuosus* in the overall meandering arrangement of the basic structural elements (Fig. 4I, J), whereas *Desmograption* follows an essentially straight or a slightly curved route (Fig. 4E, F).

Still other forms (*Lorenzina*, *Capodistria*, *Fascisichnium*) show seemingly discrete, relatively thick burrow segments arranged in a loop style ($CC \geq 8$, mostly), which are grouped into the “multiconnected loop” topological prototype (B-6, Table 1, Fig. 5D). They are potentially equipped with the branching points. For example, the reconstruction of *Lorenzina* from abundant fossil materials suggests that it is very likely a three-dimensional branched form with systematic radiating branches (Uchman 1998). The same situation may also be true for similar, regularly arranged “tubercule” and “limb” structures like *Capodistria* and *Fascisichnium* (Fig. 5B, C). However, due to the speculative nature of their three-dimensional structures, they are currently described as composed of nontouching connected components, although listed under the tree graphoglyptid group (Table 1). If further studies confirm their inherent tree or even net topology, they may possibly be redirected to the stellate, twiggy-stellate, or uniseries branch categories or to some new categories.

Topological Architecture and Prototypes of Net Graphoglyptids.—Net graphoglyptids are represented by a moderate number of ichnotaxa (17 ichnospecies, though mostly recognized by sizes, see Uchman [1995]). Although their connected component features are somewhat difficult to observe, probably



FIGURE 4. Topological architecture and prototypes of multiconnected tree graphoglyptids, the multilink linear minor group. A–J, Fossil examples of the multilink linear subgroup of tree graphoglyptids. A, *Arabesca simplex* (Seilacher, 1977), Eocene, Zarauz, northern Spain, traced from Seilacher (1977: Fig. 9a). B, *Arabesca cervicorne* (Seilacher, 1977), Eocene, Pindos, Greece, traced from Seilacher (1977: Fig. 9b). C, *Ubinia alternans* (Seilacher, 1977), Cenomanian, Lower Godula Beds, Wisła, Carpathians, Poland, UJ TF 2726. D, *Urohelminthoidea dertonensis* Sacco, 1888, lower Eocene, Beloveža Formation, Osielec, Carpathians, Poland, UJ TF 141. E, *Desmograption ichthyforme* (Macsoy, 1967), note the locally present straight connecting tunnels, Campanian–Paleocene, Ropianka Formation, Lipnica Wielka, Carpathians, Poland, UJ TF 1119. F, *Desmograption alternum* (Książkiewicz, 1977), holotype, lower Eocene, Beloveža Formation, Berest, Carpathians, Poland, UJ TF 843. G, *Helicolithus tortuosus* (Książkiewicz, 1970), note the short, straight connecting tunnels between the S-shaped burrow segments, Eocene, Fylsch del Grivo, Vemasso Quarry, NE Italy, 149P5. H, *Helicolithus tortuosus* (Książkiewicz, 1970), note the additional arc-shaped tunnel, connecting tunnels mostly not preserved, Miocene, Cingöz Formation, southern Turkey (photograph courtesy of Huriye Demircan), see Demircan and Tokar (2004: Plate 2, Fig. 3). I, *Paleomeandron elegans* Peruzzi, 1880, Campanian–Paleocene, Ropianka Formation, Lipnica Mała, Carpathians, Poland, UJ TF 220. J, *Paleomeandron rude* Peruzzi, 1880, middle Eocene, Hieroglyphic Beds, Grzechynia, Carpathians, Poland, UJ TF 138. K, Topological prototypes of the multilink linear subgroup of tree graphoglyptids (a total of three, illustrating the burrow margins of different connected components).

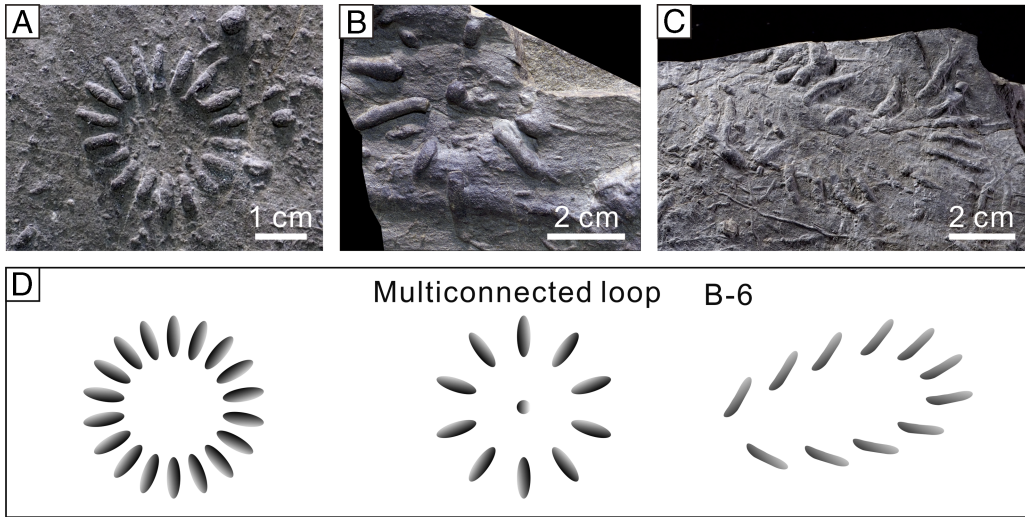


FIGURE 5. Topological architecture of the multiconnected loop topological prototype included in tree graphoglyptids with reservations. A–C, Fossil examples of the multiconnected loop topological prototype. A, *Lorenzina carpathica* (Zuber, 1910), Paleocene, Variegated Shale, Lipnica Mała, Carpathians, Poland, UJ TF 134. B, *Capodistria vettersi* Vialov, 1968, Cenomanian, Lower Godula Beds, Jaroszwice, Carpathians, Poland, UJ TF 96. C, *Fascisichnium extantum* Książkiewicz, 1968, holotype, Paleocene, Variegated Shale, Lipnica Mała, Carpathians, Poland, UJ TF 1567. D, Topological structures of the multiconnected loop topological prototype.

due to the preservational effects, net forms can be broadly classified into single- or multiconnected subgroups (Table 1, Fig. 6I). We are not able to precisely separate the ichnospecies for each topological prototype, because the recognized ichnospecies in the net graphoglyptids may be heterogeneous (i.e., include both single- and multiconnected forms, see Table 1).

Typical single-connected net forms can be found in *Megagraption irregulare* Książkiewicz, 1968, which is made of more or less straight branches well fused together at the branching points, forming large, irregular meshes (the “irregular mesh” topological prototype, N-1-1, Table 1, Fig. 6A). *Paleodictyon miocenicum* Sacco, 1886 (Fig. 6B) and some forms of *P. strozzii* (Fig. 6C) exhibit single-connected networks composed of arrays of nearly identical, hexagonal meshes, which can be properly assigned to the “regular mesh” topological prototype (N-1-2, Table 1).

In the “multiconnected network” topological prototype (N-2, Table 1, Fig. 6I), commonly several connected components can be observed ($CC \geq 2$) that interconnect in various ways to form the net topology. The major connecting styles include “sine curve apex touch,”

“right-angle touch,” “cross touch,” “overlap,” and “weaving” (Fig. 6I). As the morphology of the connected components and the combination styles between them change, a whole spectrum of network morphology can be envisaged, as evidenced by the high disparity of network morphology between different specimens (Fig. 6D–H).

Multiconnected net forms can be found in *Megagraption submontanum* (Azpeitia Moros, 1933), displaying principally sinuous connected components and the sine curve apex touch, right-angle touch, or cross-touch network construction styles (Fig. 6D). The multiconnected *Paleodictyon* is characterized by slightly sinuous and/or straight connected components, whose network formation displays a spectrum of complexity, showing the sine curve apex touch, cross-touch, overlap, and/or weaving relationships between different connected components (Fig. 6E–H). What is marvelous about the net graphoglyptids discussed in this study, especially the multiconnected *Paleodictyon*, is how the trace maker(s) manage to build such extensive, predominantly two-dimensional structures that take the form of regular network topology.

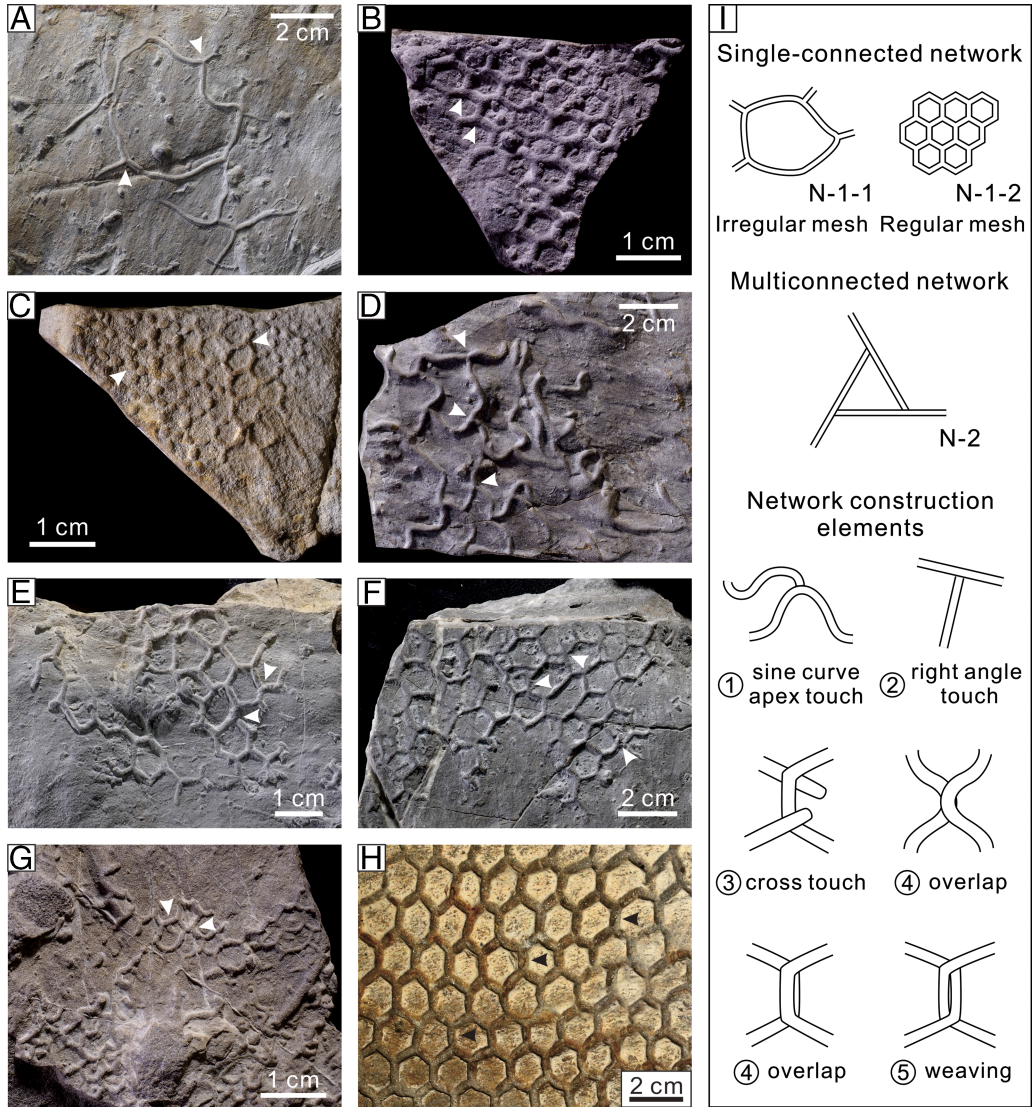


FIGURE 6. Topological architecture and prototypes of net graphoglyptids. A–H, Fossil examples of the net graphoglyptids. A–C, Single-connected network subgroup. D–H, Multiconnected network subgroup. A, *Megagraption irregulare* Książkiewicz, 1968, note the branches are well-fused at the branching points (single-connected), lower Eocene, Beloveža Formation, Lipnica Mała, Carpathians, Poland, UJTF 80a. B, *Paleodictyon miocenicum* Sacco, 1886, note the single-connected, regular hexagonal meshes, lower Eocene, Beloveža Formation, Lipnica Mała, Carpathians, Poland, UJTF 64. C, *Paleodictyon strozzii* Meneghini in Savi and Meneghini, 1850, note the single-connected hexagonal meshes and the regular arrays of tubercules, lower Eocene, Ciężkowice Sandstone, Znamyrowice, Carpathians, Poland, UJ TF 101. D, *Megagraption submontanum* (Azpeitia Moros, 1933), note the sine curve apex touch, right-angle touch, and faint cross-touch styles at burrow conjunctions, middle Eocene, Hieroglyphic Beds, Tokarnia, Carpathians, Poland, UJ TF 793. E, *Paleodictyon majus* Meneghini in Peruzzi, 1880, note the sine curve apex touch style at burrow conjunctions, lower Eocene, Beloveža Formation, Zubrzyca Górna, Carpathians, Poland, UJ TF 89a. F, *Paleodictyon majus* Meneghini in Peruzzi, 1880, note the cross-touch style at burrow conjunctions, lower Eocene, Beloveža Formation, Lipnica Mała, Carpathians, Poland, UJ TF 186. G, *Paleodictyon strozzii* Meneghini in Savi and Meneghini, 1850, note the overlapping of the undulated burrow segments, Upper Cretaceous, Sromowce Beds, Jaworki, Carpathians, Poland, UJ TF 330. H, *Paleodictyon* isp., note the weaving topology between burrow segments and tunnel thinning in the twisted part, Miocene, River Savio, Italy, on display at Museo Geologico G. Cappellini, Bologna (Hectonichnus 2016). I, The single-connected network and multiconnected network topological prototypes of net graphoglyptids, along with five types of network construction styles of the multiconnected forms (all illustrating the margins of burrow segments).

Discussion

Implications on Ichnotaxonomy from Topological Analysis.—From the topological analysis of the various line, tree, and net graphoglyptids, it is evident that they belong to contrasting internal structural categories and distinct topological prototypes. The topological analytical framework not only helps to describe the essential morphological and structural characteristics of the separate groups, but also constrains the possible construction styles for a given topological prototype. The subdivisions according to the detailed topological architecture and fabrication styles prompt certain revisions of the current ichnotaxonomical framework. Certain ichnotaxa formerly listed under the same ichnogenus, and therefore assumed to have similar morphology and function, actually show high incongruence in their detailed topological structure and constructional methods. For instance, the two-way spiral *Spirorhapse involuta* reflects significantly different construction styles from the single-spiral forms attributed to the same ichnogenus (*Spirorhapse azteca*, *S. graeca*) (Fig. 2). *Ubinia wassoeivitschi* and *U. alternans* in the tree graphoglyptid group in fact belong to the uniserial branch (B-4) and multilink linear (B-5) subgroups, respectively (Table 1, Figs. 3F and 4C). And *Helicolithus sampelayoi* is essentially a single-connected lateral spiral structure (L-5) (Fig. 2F, G), which is significantly different from *H. tortuosus* as a multiconnected tree structure made of two connected component series (B-5-3) (Table 1, Fig. 4G, H, K). The same is true for *Urohelminthoida appendiculata* (B-3) and *U. dertonensis* (B-5-2), which exhibit contrasting connected component features (Table 1, Figs. 3D and 4D).

Functional Interpretation of Line Graphoglyptids.—Single-connected line-form trace fossils of uniform burrow width (which excludes the possibility of multiple recrossing) largely represent the architecture of solitary makers, with simple functions as a relatively independent space for feeding, foraging, and/or living. Line graphoglyptids are single-connected structures with uniform tunnel diameter for a given pattern. Particularly, morphometric analysis of the meandering line graphoglyptid *Helminthorhapse* shows good correlation between the fractal dimension (indicates the space usage of

a given geometric pattern) and the meander width versus tunnel width ratio, suggesting possible increased space usage by enhancing the wall-following behavior (Fan et al. 2017). And *Cosmorhapse lobata*, with its deep and highly thigmotactic second-order meanders (Fig. 2B), and *Spirorhapse involuta* show a relatively high fractal dimension (Lehane and Ekdale 2013a, 2016), which also indicates the capability of their trace makers to cover a given surface. The space-filling ability of these ichnotaxa may be more adapted to efficient sediment feeding (i.e., pascichnia, a trace fossil ethological category denoting a combination of locomotion and feeding; see Seilacher [1953]) rather than the trapping function, although the latter possibility cannot be completely ruled out.

Functional Interpretation of Tree Graphoglyptids.—The recognition of branching points and connected components in the topological analysis aids semiquantitative functional morphological studies of trace fossils. The spatial arrangement of branching points and connected components, the basis of the subdivision of tree graphoglyptids, depicts the organization and hierarchy of the different burrow-excavation processes.

The many branches in the single-connected stellate topological prototype (B-1) share a common branching point, suggesting multiple recrossing at the point and the possible presence of a main stem tunnel connected to that branching point. The tree-like arrangement of the branching points in the single-connected twiggy-stellate topological prototype (B-2) contributes to a hierarchy of burrow components, which also possibly stem from a main tunnel, just as in the stellate subgroup. Some twiggy-stellate forms display certain self-similar features (e.g., *Chondrorhapse*) and can possibly be simulated by Lindenmayer systems (L-systems, a form of rewriting systems) (Prusinkiewicz and Lindenmayer 1990; Plotnick 2003). The single-connected uniserial branch subgroup (B-4) is similar to the stellate and twiggy-stellate subgroups (B-1 and B-2) in that it is also a centralized structure, showing a main tunnel where multiple branches protrude. The looped arrangement of the preserved burrow segments in the multiconnected loop subgroup

(B-6) is also suggestive of some radial, centralized construction styles (although their complete structures have not yet been confirmed). For *Urohelminthoida appendiculata* of the branched-zigzag topological prototype (B-3) (Fig. 3D, K), the animal is inferred to continuously shift its direction of movement and make rather tight turns at the end of the apex extensions, such that the two limbs used in the turns cannot be properly differentiated.

In the multiconnected tree graphoglyptids (B-5), it is possible to recognize multiple, repeatedly arranged connected components of uniform tunnel width that are linked to extend uni- or multidirectionally (Fig. 4). The multiple, well-defined burrow segments (connected components) of uniform diameter in a given multiconnected graphoglyptid pattern are probably produced by a series of discrete excavation events. The multiconnected tree graphoglyptids are generally small-sized, mostly between 1 and 5 mm in burrow width (Lehane and Ekdale 2016), which has previously been listed as an important feature of graphoglyptids (Miller 2014). The small tunnel diameter suggests tiny trace makers. Based on graph theory, it is speculated that *Paleodictyon* could not have been the architecture of a single animal, because the total tunnel length would greatly exceed the animal's size range if it was to traverse all the routes (Honeycutt and Plotnick 2005). The same situation may also be true of some multiconnected tree graphoglyptids such as *Desmograpton*, where the total length of the many long semiparallel tubes would be significantly larger than the tunnel width reflecting the trace-making animal's size (Fig. 4E, F). And in *Helicolithus tortuosus* and *Paleomeandron*, there is also the great linear extension in a meandering fashion of the minute "construction blocks" (Fig. 4G–J). Given the small size of the trace maker and the large surface or linear extension of the graphoglyptid galleries, entire burrow structures are generally well preserved, without significant evidence of tunnel collapse or degeneration because of desertion by the trace maker. Therefore, combining evidence from both connected component features and general morphological patterns, we find it likely that certain multiconnected tree graphoglyptids

(e.g., the two-series connected component topological prototype, B-5-3) result from the collective behaviors of a group of conspecific animals (cf. Miller 1991). There is only a low possibility that these multiconnected tree graphoglyptids represent the tunnel systems of a solitary tiny trace-making animal that toiled to make and maintain an unconventionally large "underground palace" for itself.

In the collective behavioral analytical framework, the distinct patterns (*Desmograpton*, *Helicolithus tortuosus*, *Paleomeandron*) of the two-series connected component topological prototype (B-5-3) probably belong to a common construction model. In this model, *Helicolithus tortuosus* represents forms with multiple S-shaped burrows nearly equidistantly protruding from a precedent meandering tunnel (Fig. 7A). This meandering tunnel is locally preserved as an additional component of the burrow galleries (as shown in Fig. 4H, K). The similar shape and size of all the S-shaped tubes may suggest the construction from a group of individuals at primarily the same ontogenetic or developmental stage, and their near-parallel arrangement is probably an indication of mutual avoidance in the process of simultaneous burrow excavation. *Desmograpton* can also be constructed from the precedent linear arrangement of individuals. In this case, the original individuals are probably evenly distributed along two semiparallel routes (Fig. 7A). The straight parallel limbs in *Desmograpton ichthyforme* generally show certain displacement between the neighboring limbs (Fig. 4E), which indicate possible oppositely faced extending fronts in the construction of the neighboring limbs (Fig. 7A). The regularly flexing limbs in *Desmograpton dertonensis* and *D. alternum*, similarly, can be compared with two intersected series of curved limbs with opposite directions (*Helicolithus tortuosus*-like elements) (Fig. 7A). In all the above cases, the other connected component series (i.e., the connecting tunnels between the semiparallel tubes) probably represent another set of relative independent excavation events after the parallel tube series are constructed (evidenced by elevation differences). For *Paleomeandron*, the semiparallel tubes are too short for adequate differentiation of its affinity to either the single or bilinear route model.

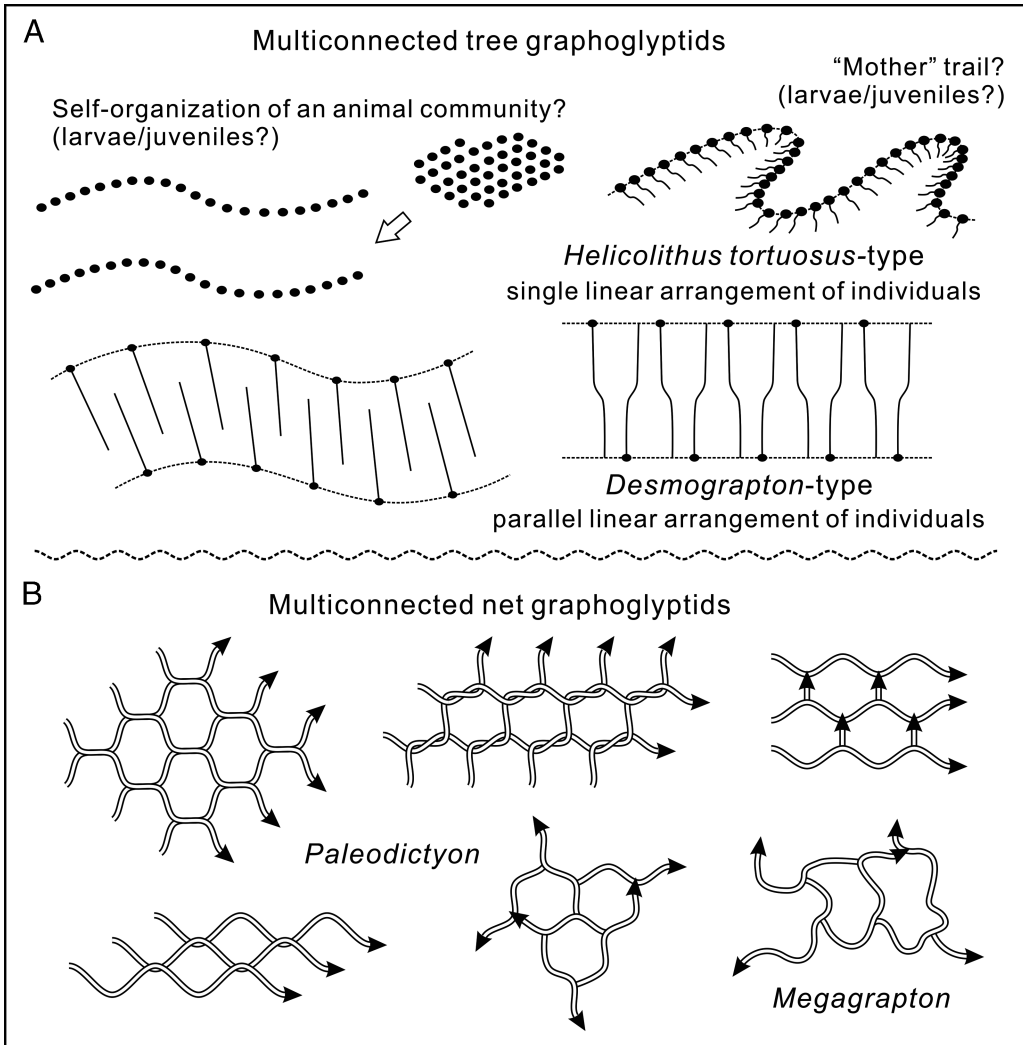


FIGURE 7. Collective behavior interpretation of multicentered tree and net graphoglyptids. A, Possible collective behavior of the two-series connected component topological prototype (B-5-3). Filled ovals indicate individual trace makers, dashed lines the arrangement routes of individuals, and solid lines the movement paths of individuals. B, Possible collective behavior of the multicentered network topological prototype (N-2). Each arrow indicates the movement path of an individual trace maker, network fabrication style of *Paleodictyon* inspired by Seilacher (1977) and observations from this study.

The overall arrangement of the burrow segments in the two-series connected component topological prototype (B-5-3) seems to be related to the size of the semiparallel tubes. In *Helicolithus tortuosus* and *Paleomeandron*, where the semiparallel tubes are relatively short, the overall arrangement could retain the meandering pattern. However, for *Desmograpton* with long semiparallel tubes, a meandering route is not possible, because the neighboring limbs would easily collide and intersect with

each other (Fig. 7A). As for the cause of the initial equidistant arrangement of the individual trace makers, there are two possibilities. One is that the individuals were laid by a particular "mother" animal along its trail (applicable to *Helicolithus tortuosus*, where the mother trail can be locally traced); the other likely explanation would be that self-organization arises among the community of individuals to create the equidistant arrangement (applicable to *Desmograpton*,

where there is no evidence of a “mother” tunnel) (Fig. 7A).

Functional Interpretation of Net Graphoglyptids.—Net graphoglyptids may be largely ascribed to two distinct types of construction styles according to their connectivity features. Irregular forms in the single-connected net graphoglyptids (irregular mesh topological prototype, N-1-1) display commonly loose networks (Fig. 6A) and are of uniform burrow diameter in a given structure, which may suggest simple network tunneling from solitary animals. The more regular, single-connected net graphoglyptids with hexagonal meshes (regular mesh topological prototype, N-1-2) are generally area-restricted and patchily distributed (e.g., Fig. 6B, C), which may also indicate solitary producers, yet with more sophisticated behaviors.

The multiconnected net graphoglyptids generally exhibit more extensive tunnel systems with small burrow width. Just like the multiconnected tree graphoglyptids, the multiconnected net graphoglyptids could similarly be interpreted as resulting from the collective behavior of conspecific animals (Fig. 7B). The uniform burrow size in a given network pattern also indicates probably similar developmental stages for the conspecific animals. The semiregular network burrow architecture, possibly from a trace-making animal community, in this case may also suggest the presence of self-organization (see Bonabeau et al. [1997] for the concept of self-organization in ethology).

Possible Producers and Paleocology of Graphoglyptids.—Single-connected line graphoglyptids (L-1 to L-4) may have been produced by solitary worms with simple behaviors (e.g., the deep-sea solitary acorn worms are responsible for *Helminthorhapha*-like meanders on the modern deep-sea floor; see Osborn et al. [2012]). Since the behavioral controls of the line-form traces (L-1 to L-4) are generally simple (Fan et al. 2017), there may be heterogeneous groups capable of producing such patterns.

Single-connected stellate graphoglyptids (B-1), in which the various rays stem from a central place where the trace maker frequently retreats (e.g., in *Estrellichnus jacaensis*), conform broadly to the scenario of an echiuran producer

(Bett et al. 1995; Przeslawski et al. 2012), but other possibilities can also be invoked (Uchman and Wetzel 2001). Single-connected twiggy-stellate graphoglyptids (B-2) are much more complex, due to the presence of a hierarchy of branches that suggest frequently migrating and tunneling animals rather than semistationary producers as in some stellate structures. The single-connected branched-zigzag structures (e.g., *Urohelminthoida appendiculata*, B-3) may represent producers that continuously shift their direction of movement through rather tight turns, a motion likely made by crustaceans that can turn their bodies flexibly (or some short-bodied worms).

Irregular, single-connected net graphoglyptids (N-1-1; e.g., *Megagraption irregulare*) may also have been produced by a myriad of animals, since such patterns do not require high behavioral capabilities. Trace fossils of similar topology have been found in a wide spectrum of environmental settings throughout the Phanerozoic (e.g., in the “horizontal branching burrow systems” architectural design of trace fossils; see Buatois et al. [2017]). The more regular single-connected net graphoglyptids (N-1-2) are still of uncertain origins, because their modern equivalents are enigmatic (modern deep-sea hexagonal structures assigned to “*Paleodictyon nodosum*,” belonging to single-connected network galleries; see Rona et al. [2009]).

Geometrically regular graphoglyptids may suggest more strict and oriented movement behaviors of the trace makers. In the shallow-marine environment, certain groups of crustaceans are able to make highly regular, single-connected tunnel systems like *Gyrolithes* and *Simusichnus* as a consequence of anatomical (biomechanical) and navigational (neurobiological) capabilities (Belaústegui et al. 2014). Particularly, *Simusichnus* galleries (although much larger) are reminiscent of some regular graphoglyptids such as *Protopaleodictyon incompositum*. Therefore, small-sized crustaceans with sophisticated construction behaviors may be tentative makers of the geometrically regular, single-connected graphoglyptids (e.g., the uniserial branch [B-4] and the lateral spiral [L-5] subgroups). The remarkably regular rosette structures (e.g., *Lorenzina*, B-6) may also have a crustacean origin. However, it should be noted

that highly ordered movement behaviors may not necessarily be restricted to a specific taxonomical group; there may be taxa with higher or lower neurobiological and biomechanical capabilities even in the same clade (e.g., in deep-sea torquaratorid acorn worms; see Priede et al. [2012]).

This is not to say that some groups of small-sized crustaceans in the deep sea cannot produce the highly regular multiconnected tree graphoglyptids (e.g., the two-series connected component topological prototype, B-5-3), but these patterns are more enigmatic due to the lack of modern analogies. However, the multiconnected net graphoglyptids (N-2) discussed in this study display a spectrum of irregularity. If the self-organized collective behavior hypothesis of multiconnected tree and net graphoglyptids is finally confirmed, crustacean producers may be a reasonable explanation, because social behaviors are readily detected in their sister group (insects) (cf. Miller 1991). Further studies in modern deep-sea biology and macrobenthic behaviors may help to further constrain the probable producers of graphoglyptids.

Traditionally, the graphoglyptids are more or less treated as a coherent functional group enacting a similar ecological role (Ekdale 1985; Seilacher 1977; Wetzel and Uchman 1998). However, given the high disparity in the architectural designs between the line, tree, and net graphoglyptids, and from the functional interpretation of the various topological prototypes of graphoglyptids noted earlier, graphoglyptids actually represent contrasting constructional methods and possibly different ecological types (cf. Lehane and Ekdale 2013b). Therefore, it is suggested that the functional and ecological analysis of graphoglyptids is best carried out at the level of detailed burrow-system morphology (e.g., topological prototypes in this study).

Conclusions

This paper made a systematic morphological characterization of all graphoglyptids (1850–2017, 79 ichnospecies from 28 ichnogenera), highlighting the topological analysis as a promising analytical tool for the taxonomy and functional interpretation of trace fossils.

The topological analysis of trace fossils consists of two steps: recognition of connected components (well-demarcated morphological units or burrow segments) and topological abstraction (abstracted burrow architecture). Three major topological groups of graphoglyptids (i.e., line, tree, and net forms) can be defined on the basis of the key topological architecture. Graphoglyptids are further attributed to 13 minor topological groups (according to the specific set of topological parameters and/or morphological details) and 19 topological prototypes (according to the variations in certain morphological details; the topological prototype is also the lowest rank in the topological classification scheme that reflects some topological *Bauplans* of a specific group of trace fossils).

Line graphoglyptids (14 ichnospecies) share the same set of topological parameters and are characterized instead by the presence or not of multiple-scale meandering and the rotation direction and orientation of the spiral burrow parts. Accordingly, they are divided into five topological prototypes (i.e., one-order meander, two-order meander, one-way spiral, two-way spiral, and lateral spiral). Line graphoglyptids are essentially single-connected structures with a uniform burrow diameter, representing primarily the feeding patterns of solitary animals.

Tree graphoglyptids are a major constructional group of graphoglyptids (48 ichnospecies) and exhibit more complex topological architectures than line forms in having more than one branching point and specific arrangement and hierarchy of the branching points and/or connected components. They are subdivided into six minor groups (i.e., stellate, twiggy stellate, branched zigzag, uniseries branch, multilink linear, and multiconnected loop) and 11 topological prototypes. Among them, the stellate, twiggy-stellate, uniseries branch, and multiconnected loop subgroups are principally centralized, single-connected structures that probably resulted from solitary animals. The branched-zigzag subgroup suggests solitary producers that could turn their bodies flexibly and make tight U-turns. The multilink linear subgroup is multiconnected and represents the most diverse category of tree graphoglyptids (20 ichnospecies). Net graphoglyptids (17 ichnospecies) are

classified into single-connected network and multiconnected network minor groups. The multiconnected net graphoglyptids are considered a continuous morphological spectrum with various combination styles of the network-forming burrow segments.

The connected components with uniform diameter in multiconnected tree and net graphoglyptids possibly represent multiple, replicated burrowing events. Backed by a couple of other lines of evidences (small and consistent burrow diameter signifying tiny trace makers, yet with great tunnel length or areal extents, and overall good preservation), it is proposed here that certain multiconnected tree and net graphoglyptids (e.g., the two-series connected component and multiconnected network topological prototypes) probably represent the emergent patterns from the collective behaviors of conspecific animals. Graphoglyptids thus provide a new perspective on the studies of solitary and collective behaviors, especially possible self-organization in animal behaviors in the deep-sea environment.

Acknowledgments

We are grateful to J. Gruza (Jagiellonian University) for helping with access to the Książkiewicz's deep-sea trace fossil collection and W. Obcowski (Jagiellonian University) for photographic work. We thank H. Demircan from the General Directorate of Mineral Research and Exploration, Ankara, for allowing us to use one of her specimen photographs. This study was supported by the National Natural Science Foundation of China (grant numbers 41290260, 41472001). The China Scholarship Council is greatly acknowledged for providing financial support to R.-Y.F. during her stay in Poland. We owe much to W. Miller, J. Lehane, and an anonymous reviewer, who provided thorough reviews, critical comments, and detailed corrections of the early versions of this paper. We acknowledge the suggestions and help from the editor S. Xiao in the publication of this paper. J. Kastigar and M. S. Curioli offered kind guidance about the style and language of the manuscript.

Literature Cited

- Azpeitia Moros, F. 1933. Datos para el estudio paleontológico del Flysch de la Costa Cantábrica y de algunos otros puntos de España. *Boletín del Instituto Geológico y Minero de España* 53:1–65.
- Belaústegui, Z., J. M. de Gibert, M. López-Blanco, and I. Bajo. 2014. Recurrent constructional pattern of the crustacean burrow *Sinusichnus sinuosus* from the Paleogene and Neogene of Spain. *Acta Palaeontologica Polonica* 59:461–474.
- Bell, J. B., D. O. B. Jones, and C. H. S. Alt. 2013. Lebensspuren of the bathyal Mid-Atlantic Ridge. *Deep-Sea Research II* 98:341–351.
- Bertling, M., S. J. Braddy, R. G. Bromley, G. R. Demathieu, J. Genise, R. Mikuláš, J. K. Nielsen, K. S. S. Nielsen, A. K. Rindsberg, M. Schirf, and A. Uchman. 2006. Names for trace fossils: a uniform approach. *Lethaia* 39:265–286.
- Bett, B. J., A. L. Rice, and M. H. Thurston. 1995. A quantitative photographic survey of “spoke-burrow” type lebensspuren on the Cape Verde Abyssal Plain. *Internationale Revue der gesamten Hydrobiologie und Hydrographie* 80:153–170.
- Bonabeau, E., G. Theraulaz, J.-L. Deneubourg, S. Aron, and S. Camazine. 1997. Self-organization in social insects. *Trends in Ecology and Evolution* 12:188–193.
- Bromley, R. G., and R. W. Frey. 1974. Redescription of the trace fossil *Gyrolithes* and taxonomic evaluation of *Thalassinoides*, *Ophiomorpha* and *Spongiomorpha*. *Bulletin of the Geological Society of Denmark* 23:311–335.
- Buatois, L. A., M. Wisshak, M. A. Wilson, and M. G. Mángano. 2017. Categories of architectural designs in trace fossils: a measure of ichnodisparity. *Earth-Science Reviews* 164:102–181.
- Danovaro, R., J. B. Company, C. Corinaldesi, G. D’Onghia, B. Galil, C. Gambi, A. J. Gooday, N. Lampadariou, G. M. Luna, C. Morigi, K. Olu, P. Polymenakou, E. Ramirez-Llodra, A. Sabbatini, F. Sardà, M. Sibuet, and A. Tselepidis. 2010. Deep-sea biodiversity in the Mediterranean Sea: the known, the unknown, and the unknowable. *PLoS ONE* 5:e11832.
- Demircan, H., and V. Toker. 2004. Cingöz formasyonu doğu yelpaze iz fosilleri (KB Adana). *Maden Tetkik ve Arama Dergisi* 129:69–87.
- Durden, J. M., E. Simon-Lledo, A. J. Gooday, and D. O. B. Jones. 2017. Abundance and morphology of *Paleodictyon nodosum*, observed at the Clarion-Clipperton Zone. *Marine Biodiversity* 47:265–269.
- Ekdale, A. A. 1980. Graphoglyptid burrows in modern deep-sea sediment. *Science* 207:304–306.
- . 1985. Paleoeology of the marine endobenthos. *Palaeogeography, Palaeoclimatology, Palaeoecology* 50:63–81.
- Fan, R.-Y., A. Uchman, and Y.-M. Gong. 2017. From morphology to behaviour: quantitative morphological study of the trace fossil *Helminthorhapha*. *Palaeogeography, Palaeoclimatology, Palaeoecology* 485:946–955.
- Farrés, F. 1967. Los “*Dendrotichnium*” de España. *Notas y Comunicaciones Instituto Geológico y Minero de España* 94:29–36.
- Fuchs, T. 1895. Studien über Fucoiden und Hieroglyphen. *Denkschriften der Kaiserlichen Akademie der Wissenschaften, Mathematisch-Naturwissenschaftliche Classe* 62:369–448.
- Fürsich, F. T., J. Taheri, and M. Wilmsen. 2007. New occurrences of the trace fossil *Paleodictyon* in shallow marine environments: examples from the Triassic–Jurassic of Iran. *Palaios* 22:408–416.
- Gaillard, C. 1991. Recent organism traces and ichnofacies on the deep-sea floor off New Caledonia, Southwestern Pacific. *Palaios* 6:302–315.
- Gong, Y.-M., and D.-H. Huang. 1997. Topologic configuration of a graphoglyptid and its functional morphologic analysis. *Chinese Science Bulletin* 42:1394–1397.
- Gong, Y.-M., and Y.-L. Si. 1991. Trace fossils and topology. *Chinese Science Bulletin* 36:1803–1806.

- . 2002. Classification and evolution of metazoan traces at a topological level. *Lethaia* 35:263–274.
- Grossgeim, V. A. 1946. O znachenii i metodike izucheniya hieroglifov (na materiale kavkazskogo flyscha). *Izvestia Akademii Nauk SSSR, Seria Geologicheskaya* 2:111–120.
- . 1961. Niekatoriye noviy hieroglifi iz nizhniemelovikh otlozheniy severo-zapodnokho Kavkaza. *Trudy Krasnodarskogo Filial'a Vsesoyuznogo Neftegazovogo Nauchno-Issledovatskogo Instituta* 6:202–206.
- Hectonichnus [Wikipedia user name]. 2016. *Paleodictyon* from Miocene of River Savio, Italy—on display at Museo Geologico G. Cappellini, Bologna. <https://upload.wikimedia.org/wikipedia/commons/9/96/Palaedictyon.JPG> (CC BY-SA 4.0 [http://creativecommons.org/licenses/by-sa/4.0] or GFDL [http://www.gnu.org/copyleft/fdl.html], via Wikimedia Commons [accessed 17/09/05]).
- Heer, O. 1877. *Flora Fossilis Helvetiae. Die vorweltliche Flora der Schweiz*. J. Würster & Co., Zürich.
- Heezen, B. C., and C. D. Hollister. 1971. *The face of the deep*. Oxford University Press, New York.
- Honeycutt, C. E., and R. E. Plotnick. 2005. Mathematical analysis of *Paleodictyon*: a graph theory approach. *Lethaia* 38: 345–350.
- Huang, D.-H., and Y.-M. Gong. 1998. Morphological-structural analysis and topologic taxonomy on trace fossils. *Science in China Series D: Earth Sciences* 41:269–276.
- Huckriede, R. 1952. Eine spiralförmige Lebensspur aus dem Kulmkieselschiefer von Biedenkopf an der Lahn (*Spirodesmos archimedeus* n. sp.). *Paläontologische Zeitschrift* 26:175–180.
- Koy, K. A., and R. E. Plotnick. 2007. Theoretical and experimental ichnology of mobile foraging. Pp. 428–441 in W. Miller III, ed. *Trace fossils: concepts, problems, prospects*. Elsevier, Amsterdam.
- . 2010. Ichnofossil morphology as a response to resource distribution: insights from modern invertebrate foraging. *Palaeogeography, Palaeoclimatology, Palaeoecology* 292: 272–281.
- Książkiewicz, M. 1968. On some problematic organic traces from the Flysch of the Polish Carpathians. *Rocznik Polskiego Towarzystwa Geologicznego* 38:1–17.
- . 1970. Observations on the ichnofauna of the Polish Carpathians. In T. P. Crimes, and J. C. Harper, eds. *Trace fossils*. Geological Journal, Special Issue 3:283–322. Seel House, Liverpool.
- . 1977. Trace fossils in the flysch of the Polish Carpathians. *Palaeontologia Polonica* 36:1–208.
- Lehane, J. R., and A. A. Ekdale. 2013a. Fractal analysis of graphoglyptid trace fossils. *Palaio* 28:23–32.
- . 2013b. Pitfalls, traps, and webs in ichnology: traces and trace fossils of an understudied behavioral strategy. *Palaeogeography, Palaeoclimatology, Palaeoecology* 375:59–69.
- . 2014. Analytical tools for quantifying the morphology of invertebrate trace fossils. *Journal of Paleontology* 88:747–759.
- . 2016. Morphometric analysis of graphoglyptid trace fossils in two dimensions: implications for behavioral evolution in the deep sea. *Paleobiology* 42:317–334.
- Macsotay, O. 1967. Huellas problematicas y su valor paleoecológico en Venezuela. *Geos* 16:7–79.
- Miller, W., III. 1991. Paleocology of graphoglyptids. *Ichnos* 1:305–312.
- . 2012. On the doctrine of ichnotaxonomic conservatism: the differences between ichnotaxa and biotaxa. *Neues Jahrbuch für Geologie und Paläontologie, Abhandlungen* 265:295–304.
- . 2014. Mystery of the graphoglyptids. *Lethaia* 47:1–3.
- Minter, N. J., L. A. Buatois, S. G. Lucas, S. J. Braddy, and J. A. Smith. 2006. Spiral-shaped graphoglyptids from an Early Permian intertidal flat. *Geology* 34:1057–1060.
- Monaco, P. 2008. Taphonomic features of *Paleodictyon* and other graphoglyptid trace fossils in Oligo-Miocene thin-bedded turbidites, northern Apennines, Italy. *Palaio* 23:667–682.
- Olivero, E. B., M. I. López Cabrera, N. Malumíán, and P. J. Torres Carbonell. 2010. Eocene graphoglyptids from shallow-marine, high-energy, organic-rich, and bioturbated turbidites, Fuegian Andes, Argentina. *Acta Geologica Polonica* 60:77–91.
- Osborn, K. J., L. A. Kuhnz, I. G. Priede, M. Urata, A. V. Gebruk, and N. D. Holland. 2012. Diversification of acorn worms (Hemichordata, Enteropneusta) revealed in the deep sea. *Proceedings of the Royal Society of London B* 279:1646–1654.
- Peruzzi, D. G. 1880. Osservazioni sui generi *Paleodictyon* e *Paleomeandron* dei terreni cretacei ed eocenici dell'Appennino settentrionale e centrale. *Atti della Società Toscana di Scienze Naturali Residente in Pisa, Memorie* 5:3–8.
- Plotnick, R. E. 2003. Ecological and L-system based simulations of trace fossils. *Palaeogeography, Palaeoclimatology, Palaeoecology* 192:45–58.
- Priede, I. G., K. J. Osborn, A. V. Gebruk, D. Jones, D. Shale, A. Rogacheva, and N. D. Holland. 2012. Observations on torquatorid acorn worms (Hemichordata, Enteropneusta) from the North Atlantic with descriptions of a new genus and three new species. *Invertebrate Biology* 131:244–257.
- Prusinkiewicz, P., and A. Lindenmayer. 1990. *The algorithmic beauty of plants*. Springer, New York.
- Przeslawski, R., K. Dundas, L. Radke, and T. J. Anderson. 2012. Deep-sea Lebensspuren of the Australian continental margins. *Deep-Sea Research I* 65:26–35.
- Ramirez-Llodra, E., A. Brandt, R. Danovaro, B. De Mol, E. Escobar, C. R. German, L. A. Levin, P. Martinez Arbizu, L. Menot, P. Buhl-Mortensen, B. E. Narayanaswamy, C. R. Smith, D. P. Tittensor, P. A. Tyler, A. Vanreusel, and M. Vecchione. 2010. Deep, diverse and definitely different: unique attributes of the world's largest ecosystem. *Biogeosciences* 7:2851–2899.
- Rex, M. A., R. J. Etter, J. S. Morris, J. Crouse, C. R. McClain, N. A. Johnson, C. T. Stuart, J. W. Deming, R. Thies, and R. Avery. 2006. Global bathymetric patterns of standing stock and body size in the deep-sea benthos. *Marine Ecology Progress Series* 317:1–8.
- Rona, P. A., A. Seilacher, C. de Vargas, A. J. Gooday, J. M. Bernhard, S. Bowser, C. Vetrani, C. O. Wirsen, L. Mullineaux, R. Sherrell, J. F. Grassle, S. Low, and R. A. Lutz. 2009. *Paleodictyon nodosum*: a living fossil on the deep-sea floor. *Deep-Sea Research II* 56:1700–1712.
- Sacco, F. 1886. Intorno ad alcune impronte organiche dei terreni terziari del Piemonte. *Atti della Reale Accademia delle Scienze di Torino* 21:687–710.
- . 1888. Note di Paleocinologia Italiana. *Atti della Società Italiana di Scienze Naturali* 31:151–192.
- Savi, P., and G. G. Meneghini. 1850. Osservazioni stratigrafiche e paleontologiche concernenti la geologia della Toscana e dei paesi limitrofi. Appendix. Pp. 246–528 in R. I. Murchison, ed. *Memoria sulla struttura geologica delle Alpi, degli Appennini e dei Carpazi*. Stamperia Granducale, Firenze.
- Seilacher, A. 1953. Studien zur Palichnologie. I. Über die Methoden der Palichnologie. *Neues Jahrbuch für Geologie und Paläontologie, Abhandlungen* 96:421–452.
- . 1962. Paleontological studies on turbidite sedimentation and erosion. *Journal of Geology* 70:227–234.
- . 1977. Pattern analysis of *Paleodictyon* and related trace fossils. In T. P. Crimes, and J. C. Harper, eds. *Trace fossils 2*. Geological Journal, Special Issue 9:289–334. Seel House, Liverpool.
- . 1989. *Spirocormorphaphe*, a new graphoglyptid trace fossil. *Journal of Paleontology* 63:116–117.
- Sims, D. W., A. M. Reynolds, N. E. Humphries, E. J. Southall, V. J. Wearmouth, B. Metcalfe, and R. J. Twitchett. 2014. Hierarchical random walks in trace fossils and the origin of optimal search

- behavior. *Proceedings of the National Academy of Sciences USA* 111:11073–11078.
- Stefani, C. de. 1895. Aperçu géologique et description paléontologique de l'île de Karpathos. Pp. 165–180 in C. de Stefani, C. J. Forsyth Major, and W. Barbey, eds. *Karpathos. Étude géologique, paléontologique et botanique*. Georges Bridel & Cie Éditeurs, Lausanne.
- Uchman, A. 1995. Taxonomy and palaeoecology of flysch trace fossils: the Marnoso–arenacea Formation and associated facies (Miocene, Northern Apennines, Italy). *Beringeria* 15:3–115.
- . 1998. Taxonomy and ethology of flysch trace fossils: revision of the Marian Książkiewicz collection and studies of complementary material. *Annales Societatis Geologorum Poloniae* 68:105–218.
- . 1999. Ichnology of the Rhenodanubian Flysch (Lower Cretaceous–Eocene) in Austria and Germany. *Beringeria* 25:67–173.
- . 2001. Eocene flysch trace fossils from the Hecho Group of the Pyrenees, northern Spain. *Beringeria* 28:3–41.
- . 2003. Trends in diversity, frequency and complexity of graphoglyptid trace fossils: evolutionary and palaeoenvironmental aspects. *Palaeogeography, Palaeoclimatology, Palaeoecology* 192:123–142.
- . 2004. Phanerozoic history of deep-sea trace fossils. In D. McIlroy, ed. *The application of ichnology to palaeoenvironmental and stratigraphic analysis*. Geological Society of London Special Publication. 228:125–139.
- Uchman, A., and A. Wetzel. 2001. *Estrellichmus jacaensis* nov. igen., nov. isp.—a large radial trace fossil from Eocene flysch (Hecho Group, northern Spain). *Geobios* 34:357–361.
- Uchman, A., N. E. Janbu, and W. Nemeček. 2004. Trace fossils in the Cretaceous–Eocene flysch of the Sinop–Boyabat Basin, Central Pontides, Turkey. *Annales Societatis Geologorum Poloniae* 74:197–235.
- Uchman, A., N. Abbassi, and M. Naeefi. 2005. *Persichmus* igen. nov. and associated ichnofossils from the Upper Cretaceous to Eocene deep-sea deposits of the Sanandaj Area, West Iran. *Ichnos* 12:141–149.
- Ulrich, E. O. 1904. Fossils and age of the Yakutat Formation. Description of the collections made chiefly near Kodiak, Alaska. Pp. 125–146 in B. K. Emerson, C. Palache, W. H. Dall, E. O. Ulrich, and F. H. Knowlton, eds. *Alaska, geology and paleontology*. Doubleday, Page & Co, New York.
- Van der Marck, W. 1863. Fossile Fische, Krebse und Pflanzen aus dem Plattenkalk der jüngsten Kreide in Westphalen. *Palaeontographica* 11:1–83.
- Vialov, O. S. 1968. O zvezdchatykh problematikakh. *Ezhegodnik Vsesoyuznogo Paleontologicheskogo Obshchestva* 18:326–340.
- . 1971. Redkie problematiki iz Mezozoya Pamira i Kavkaza. *Paleontologicheskii Sbornik* 7:85–93.
- Wetzel, A., and A. Uchman. 1998. Deep-sea benthic food content recorded by ichnofabrics: a conceptual model based on observations from Paleogene flysch, Carpathians, Poland. *Palaios* 13:533–546.
- Wetzel, A., and R. G. Bromley. 1996. Re-evaluation of the ichnogenus *Helminthopsis*—a new look at the type material. *Palaeontology* 39:1–19.
- Zuber, R. 1910. Eine fossile Meduse aus dem Kreideflysch der ostgalizischen Karpathen. *Verhandlungen der Kaiserlich-Königlichen Geologischen Reichsanstalt* volume for year 1910:57–58.